Lithium isotopes in dolostone as a palaeo-environmental proxy – An experimental approach

Holly L. Taylor[1], Isaac J. Kell Duivestein[2], Juraj Farkas[3,4], Martin Dietzel[2], and Anthony Dosseto[1]

[1]Wollongong Isotope Geochronology Laboratory. School of Earth, Atmospheric and Life Sciences. University of Wollongong. Wollongong, NSW, Australia
[2]Institute of Applied Geosciences. Graz University of Technology. Graz, Austria
[3]Department of Earth Sciences. University of Adelaide. Adelaide, SA, Australia
[4]Department of Environmental Geosciences, Czech University of Life Sciences, Prague, Czech Republic

Correspondence: Holly Taylor (hlt434@uowmail.edu.au)

1   **Abstract.** Lithium (Li) isotopes in marine carbonates have considerable potential as a proxy to constrain past changes in
2   silicate weathering fluxes and improve our understanding of Earth's climate. To date the majority of Li isotope studies on
3   marine carbonates have focussed on calcium carbonates. Determination of the Li isotope fractionation between dolomite and
4   a dolomitizing fluid, would allow us to extend investigations to deep times (i.e., Precambrian) when dolostones were the
5   most abundant marine carbonate archives. Dolostones often contain a significant proportion of detrital silicate material, which
6   dominates the Li budget, thus pre-treatment needs to be designed so that only the isotope composition of the carbonate-
7   associated Li is measured. This study aims to serve two main goals: (1) determining the Li isotope fractionation between
8   Ca-Mg carbonates and solution and (2) to develop a method for leaching the carbonate-associated Li out of dolostone while
9   not affecting that contained within the detrital portion of the rock. We synthesized Ca-Mg carbonates at high temperature (150
10 to 220 °C) and measured the Li isotope composition (δ^7Li) of precipitated solids and their respective reactive solutions. The
11 relationship of the Li isotope fractionation factor with temperature was obtained:

12 $$10^3 . ln\alpha_{prec-sol} = -((2.56 \pm 0.27).10^6)/T^2 + (5.8 \pm 1.3) \tag{1}$$

13 Competitive nucleation and growth between dolomite and magnesite were observed during the experiments, however, with-
14 out notable effect of their relative proportion on the apparent Li isotope fractionation. We found that Li isotope fractionation
15 between precipitated solid and solution is higher for Ca-Mg carbonates than for Ca carbonates. If the temperature of a precipi-
16 tating solution is known or can be estimated independently, the above equation could be used in conjunction with the Li isotope
17 composition of dolostones to derive that of the solution and hence make inferrals about the past Li cycle. In addition, we also
18 conducted leaching experiments on a Neoproterozoic dolostone and a Holocene coral. Results show that leaching with 0.05M
19 HCl or 0.5 % acetic acid at room temperature for 60 min releases Li from the carbonate fraction without significant contribution
20 of Li from the siliciclastic detrital component. These experimental and analytical developments provide a basis for the use of
21 Li isotopes in dolostones as a palaeo-environmental proxy, which will contribute to further advance our understanding of the
22 evolution of Earth's surface environments.

24 1   Introduction

25 Lithium isotopes in marine carbonates have emerged as a powerful proxy to understand the evolution of the ocean chemistry,
26 past silicate weathering fluxes and their links to global climate. Application to calcium carbonates (e.g. foraminifera, limestone)
27 has shed some light on hotly debated topics such as, the evolution of Earth's climate during the Cenozoic (Misra and Froelich,
28 2012; Li et al., 2014; Wanner et al., 2014; Vigier and Goddéris, 2015; Hathorne and James, 2006), oceanic anoxic events
29 (Pogge von Strandmann et al., 2013; Lechler et al., 2015) and Palaeozoic glaciation (Pogge von Strandmann et al., 2017).
30 Although post-depositional alteration can play an important role in the formation of dolomite (Geske et al., 2012; Burns et al.,
31 2000), the application of Li isotopes to marine dolostone could help to extend our understanding of the geochemical evolution
32 of ancient dolomitizing solutions, particularly in early Earth geological history (i.e., Precambrian).

33 While data of Li isotopic fractionation during calcite precipitation has been relatively well constrained (Marriott et al.,
34 2004a, b; Dellinger et al., 2018), there is currently no data available pertaining to Li isotope fractionation during dolomite
35 formation. Therefore in this study, precipitation experiments were carried out at various temperatures (150 – 220 °C), where
36 the Li isotopic composition of the precipitated solids and their respective reactive solutions were subsequently measured in
37 order to determine the fractionation factor between the fluid and solid phases. The experiments were conducted at elevated
38 temperatures due to the impossibility of synthesizing well-ordered dolomite at ambient temperatures on a laboratory time scale
39 (Land, 1998; Arvidson and Mackenzie, 1999; Gregg et al., 2015).

40 One major difficulty with interpreting Li isotopes in dolostone is that they often contain a significant proportion of silici-
41 clastic material (e.g. detrital micas and/or authigenic clay minerals). The abundance of Li in silicate minerals is higher than in
42 carbonates (typically more than two orders of magnitudes), thus sample pre-treatment must be undertaken to extract Li from
43 only the carbonate fraction (Pogge von Strandmann et al., 2013; Bastian et al., 2018). Therefore, in this study we have tested
44 various pre-treatment methods in order to refine a procedure that faithfully yields the isotopic composition of the carbonate-
45 associated Li fraction in dolostones exclusively.

46 2   Methods

47 2.1   Ca-Mg carbonate synthesis

48 Synthesis of Ca-Mg carbonates was conducted in Teflon-lined, stainless steel autoclaves at temperatures of 150, 180 and
49 220 °C $\pm$ 5 °C) through the reaction of $\sim$300 mg of powdered inorganic aragonite (speleothem aragonite; in-house mineral
50 collection at Graz University of Technology) with an artificial brine solution containing 200 mM Mg, 0.245 mM Li and 50
51 mM NaHCO$_3$. The reactive fluid was prepared by dissolving analytical grade MgCl$_2$.6H$_2$O (Roth; $\geq$ 99 %, p.a, ACS), LiCl
52 (Merck; $\geq$ 99 %, ACS, Reag. Ph Eur) and NaHCO$_3$ (Roth; $\geq$ 99.5 %, p.a., ACS, ISO) in ultrapure water (Millipore Integral 3:
53 18.2 MΩ.cm-1). The stock solution was subsequently filtered through a 0.45 μm cellulose acetate membrane filter (Sartorius).

54 The reagent inorganic aragonite was milled to a grain size < 20 μm using a vibratory mill (McCrone Micronizing Mill) for
55 10 minutes and collected by dry sieving prior to use in the experiments. Autoclaves were sealed immediately after mixing the
56 inorganic aragonite with the appropriate volume of stock solution and placed in preheated ovens. Samples were taken from the
57 autoclaves at each operating temperature after a given reaction time (Table 1), including repeat samples. Upon removal from
58 heat, the reactors were quenched and the samples were subsequently filtered through a 0.2 μm cellulose acetate membrane
59 (Sartorius) using a vacuum filtration unit. Samples were then thoroughly rinsed with ultrapure water (Millipore Integral 3: 18.2
60 MΩ ·cm-1) to remove any soluble salts from the matrix and subsequently dried in an oven at 40 °C overnight to be ready
61 for solid phase analysis. An aliquot of the reactive fluid was acidified to a $\sim$3 % HNO_3 matrix for elemental and Li isotope
62 analyses using Merck® Suprapur™ HNO_3.

2.2 Leaching experiments

64 A Neoproterozoic dolostone from the Nuccaleena Formation (Flinders Ranges, South Australia, $\sim$635 Ma) and a Holocene
65 *Porites* coral were used to evaluate the effect of different leaching protocols on the measured Li isotope composition. Sam-
66 ples were ground to a powder using a TEMA chromium-ring grinding mill. An aliquot of powdered dolostone was used for
67 mineralogy quantification performed using X-ray diffraction. Another aliquot of one gram was placed in a clean polypropylene
68 centrifuge tube and 20 mL of solution was added. Leaching was tested with hydrochloric acid (HCl) of varying concentrations
69 (0.05M, 0.1M, 0.15M, 0.2M, 0.3M, 0.5, 0.8M, 1M, 6M) and acetic acid (HAc) at concentrations of 0.5 and 2 %. Acetic acid
70 and HCl solutions were prepared from trace grade glacial acetic acid (Merck® Suprapur™) and ultra-trace grade 30 % HCl
71 (Merck® Ultrapur™). In each case, the powder and solution reacted at room temperature for one hour, while continuous mix-
72 ing was achieved with an orbital shaker. The supernatant fluid was separated by centrifugation at 4000 rpm for 15 minutes.
73 After separation, the supernatant fluid was extracted using acid-washed disposable pipettes. An aliquot containing $\sim$60 ng of
74 Li was subsequently sampled for cation exchange chromatography.

2.3 Mineralogy quantification

76 Quantitative phase contents of the synthesized solids were determined by powder X-ray diffraction (XRD) of finely ground
77 aliquots performed on a PANalytical X'Pert PRO diffractometer outfitted with a Co-target tube (operated at 40 kV and 40 mA),
78 a high-speed Scientific X´Celerator detector, 0.5 °antiscattering and divergence slits, spinner stage, primary and secondary
79 soller and automatic sample changer. Samples were finely ground by hand using a mortar and pestle prior to analysis and were
80 loaded in a random orientation using the top loading technique. The samples were analysed over the range $4 - 85°2\theta$ with a
81 step size of $0.008°2\theta$ and a count time of 40 seconds/step. Mineral quantification was obtained by Rietveld Refinement of the
82 XRD patterns using the PANalytical X'Pert HighScore Plus Software and its implemented pdf-2 database.

2.4 Elemental concentrations

Lithium concentrations of solutions were analysed in acidified (0.3 M HNO$_3$) aliquots by inductively coupled plasma optical emission spectroscopy (ICP-OES) using a PerkinElmer Optima 8300. A range of in-house and NIST 1640a standards were measured at the beginning and end of a sample series, with an estimated analytical error (2 σ, 3 replicates) of $\pm$ 3% relative to the standard. For synthesized solids, an aliquot of each precipitate was dissolved in 0.9 M HNO$_3$ at 70 °C for 12 hours in an ultrasonic bath to ensure complete digestion. Subsequently Li concentrations were analysed by ICP-OES following the same method as for the aqueous solutions.

2.5 Lithium isotopes

Sample preparation for Li isotope measurement was undertaken in a Class 100 cleanroom at the Wollongong Isotope Geochronology Laboratory, University of Wollongong. For mineral precipitates, the samples were ground using a mortar and pestle before aliquots of <0.05 g were weighed. The sample aliquots were dissolved in dilute HNO$_3$ (Ultrapur™) and 0.2 mL of concentrated H$_2$O$_2$ (31 % Ultrapur™) was added to ensure the breakdown of organics.

The samples were then placed on a hotplate overnight at 50 °C to reflux and ensure complete digestion of the solids. After complete digestion of the solids, Li concentrations were measured by Quadrupole ICP-MS. An aliquot of the digested samples containing $\sim$ 60 ng of Li was then dried down and taken up into 1.5 mL of Ultrapur™ 1 M HCl. Samples were then treated with a two-step cation exchange chromatography procedure, following the methods of Balter and Vigier (2014) to separate Li from the sample matrix. For Li isotope measurements it is crucial that 100 % of Li is recovered from the cation exchange columns as δ^7Li compositions have been shown to vary by up to $\sim$ 200 ‰ during chromatography due to incomplete recovery (Pistiner and Henderson, 2003). It is also crucial to remove elements such as Na and Ca as large amounts of Ca can coat the cones of the mass spectrometer while Na can reduce Li ionisation in the plasma, and cause further Li isotopic fractionation during analysis (James and Palmer, 2000). For chromatography, 30 mL Savillex micro columns (6.4 mm internal diameter, 9.6 cm outside diameter, 25 cm capillary length) were used together with Biorad AG50W-X8 resin as the cation exchange medium (volume = 3.06 cm^3). The columns were calibrated with seawater prior to treating the samples to verify that the procedure yielded 100 % of the Li (Table A1). The columns were cleaned with 30 mL of 6M HCl, rinsed with 2 mL of MilliQ™ water and conditioned using 8 mL of titrated, 1 M Ultrapur™ HCl before sample loading. To ensure the complete removal of interfering elements from the Li, samples were passed through the columns twice; after the first elution, the samples were dried down, taken up in 1 M HCl and reloaded into the columns. The Li elutions were dried down and subsequently re-dissolved in Ultrapur™ 0.3M HNO$_3$ ready for isotopic analysis. Lithium isotope ratios were measured by multi collector inductively coupled plasma mass spectrometry (MC ICP-MS) on a ThermoFisher Neptune Plus at the Wollongong Isotope Geochronology Laboratory, University of Wollongong. A 30 ppb solution of IRMM-16 Li isotopic standard was used at the start of each measurement session to tune the instrument. An intensity of $\sim$1 V was routinely obtained for ^{7}Li, while the background ^{7}Li intensity was between 5-30 mV. During analysis, standard bracketing, using IRMM-16 as the primary standard, was applied to correct the measured ^{7}Li/^{6}Li values for mass bias (Flesch et al., 1973). Instrumental blanks were measured before each sample so that

116 background signal could be accounted for. The $^7Li/^6Li$ ratios were converted to δ^7Li values using L-SVEC as reference to
117 (Carignan et al., 2007) (Eq.(2)).

118 $\delta^7 Li = ((^7Li/^6Li)_{sample}/(^7Li/^6Li)_{L-SVEC}) - 1 \times 1000$ (2)

119   The accuracy of analysis was assessed using synthetic solutions Li6-N and Li7-N (Carignan et al., 2007) as secondary
120 standards every 6 samples. The accuracy of chromatography and analysis was assessed using a seawater standard (Table A1).
121 External uncertainty on δ^7Li compositions (at 2 σ level) was evaluated by measurement of precipitated solids and solutions
122 from repeat experiments at 150 °C (n = 3) and 180 °C (n = 2), amounting to 0.86 ‰ for precipitated solids and 1.2 ‰ for
123 solutions.

124 3 Results

125 3.1 Precipitation experiments

126 Synthesized minerals are comprised of dolomite and magnesite (Table 1); their relative amount shows a relationship with
127 temperature, with higher reaction temperatures yielding more magnesite and less dolomite compared to lower temperatures
128 (Fig. 1). The Li concentration of reactive solutions ranges from 1,666 to 3,695 μg.L^{-1} (Table A2) and shows no correlation
129 with reaction temperature. On the contrary, the Li concentration of precipitated solids are consistent with (Marriott et al., 2004a,
130 b) as it decreases with increasing temperature (from 25.9 to 8.20 ppm; Table A2).
131   The δ^7Li of the initial reactive solution is 7.85 ‰ (Table 2). After reaction the δ^7Li value of the solution (δ^7Li_{sol}) vary
132 between 7.87 and 9.48 ‰, while the δ^7Li values in the precipitated solid (δ^7Li_{prec}) range from -0.63 to 3.08 ‰ (Table 2).
133 The precipitated solids are 4.79 to 8.6 ‰ lighter than the solution, and this difference (termed $10^3.ln\alpha_{prec-sol}$) increases with
134 decreasing temperature (Table 2).
135   The Li isotope fractionation factor between the precipitated solid and the solution (calculated as $10^3.ln\alpha_{prec-sol} = 10^3.ln(1000+$
136 $\delta^7Li_{prec}/1000 + \delta^7Li_{sol})$ displays values within error of each other, despite a wide range of concentrations of dolomite or
137 magnesite precipitated (Fig. 2). Similarly, there is no relationship between the Li distribution coefficient between precipitated
138 solid and solution ($D_{[Li]prec-sol} = [Li]_{prec}/[Li]_{sol}$, where $[Li]_{prec}$ and $[Li]_{sol}$ are the Li concentrations in the precipitated
139 solid and the solution, respectively), and mineral abundances (Fig. 3). Conversely, there is a positive relationship between
140 $10^3.ln\alpha_{prec-sol}$ and the reaction temperature (Fig. 4).

141 3.2 Leaching experiments

142 For the dolostone, δ^7Li values of the leaching solution decrease from 9.5 to 4.0 ‰, with increasing HCl concentration (Table
143 3; Fig. 5a). The molar Al/Mg ratio in the leaching solutions increases at HCl concentrations >0.8 M from ~0.0009 to 0.01
144 (Fig. 5b). The leaching solutions show an increase in molar Li/Ca ratio from 6.3x10^{-6} to 25x10^{-6} with decreasing δ^7Li
145 (Fig. 6a). Furthermore, the molar Li/Mg ratio increases from 5 to 12x10^{-5} with increasing δ^7Li (Fig. 6b). Very little carbonate

146 minerals other than dolomite (1.1 wt % calcite and 2.1 wt % ankerite) are present in the dolostone sample, and the silicate

147 minerals represents ∼26 wt % of the sample (14 wt % quartz, 6.2 wt % muscovite and 5.1 wt % albite) (Table A3). Leaching

148 with acetic acid yields δ^7Li compositions in the solution similar to values observed in very dilute HCl (Fig. 7). The δ^7Li of the

149 2 % HAc leaching solution is lower than that of the 0.5 % HAc leaching solution.

150 For the Holocene coral, the sample is dominated by aragonite (Table A4) and the leaching solution shows a similar trend to

151 that from the dolostone leaching experiment, with δ^7Li values decreasing from 20.1 to 16.9 ‰ with increasing HCl concentra-

152 tion (Table 3; Fig. 8). Total dissolution of the coral yields a δ^7Li value in the solution of 20.6 ‰, which is within error of the

153 values determined for HCl leaching experiments with acid concentrations <0.5 M (Table 3).

154 4 Discussion

155 4.1 Lithium isotope fractionation during inorganic precipitation of Ca-Mg carbonate

156 The precipitated solids of the synthesis experiments consist of Mg-Ca carbonates with variable amounts of dolomite (CaMg(CO$_3$)$_2$)

157 and magnesite (MgCO$_3$) (Table 1). The δ^7Li composition of the precipitated solid is systematically isotopically lighter than

158 that of the reactive solution (Table 2). These results are consistent with previous experimental work on Li isotope fractionation

159 during calcite precipitation (Marriott et al., 2004a, b), which showed that the Li isotope composition of calcite is isotopically

160 lighter than that of the corresponding fluid. Teng et al. (2008) have suggested that the incorporation of ^{6}Li over ^{7}Li in minerals

161 compared to the growth solution reflects a change from four- to six-fold coordination of Li during mineral growth. In calcite

162 from foraminifera and aragonite from corals, δ^7Li values are respectively about 3 and 11 ‰ lower compared to their growth

163 solutions (Marriott et al., 2004a). Here, the precipitated minerals are 4.8 to 8.6 ± 0.6 ‰ (1 σ; n=3) lighter than the solution

164 over all temperatures (150, 180 and 220 °C). This difference increases with decreasing temperature, as would be expected

165 for stable isotope fractionation at equilibrium. As our experiments were conducted at high temperatures (150, 180 and 220

166 °C), the system can be reasonable considered to be approaching isotope equilibrium conditions as fractionation scales with

167 the inverse of reaction temperature (see Fig. 3). Marriott et al. (2004a) suggested that Li isotope fractionation probably occurs

168 at equilibrium even at lower temperatures for several reasons: (i) kinetic fractionation would probably be much greater (up to

169 ∼80 ‰) than that observed (both in calcite and in Ca-Mg carbonate), thus requiring boundary layer processes or the presence

170 of a back-reaction, for which there is no evidence. (ii) Observed isotopic fractionation between calcite and growth solution, as

171 well as between Ca-Mg carbonate and growth solution, are consistent with ab initio calculations for equilibrium fractionation

172 (Kazuyo Yamaji et al., 2001). (iii) Lithium isotope fractionation between calcite and growth solution is relatively constant

173 across a wide range of concentration of Li incorporated in calcite (this was not tested here).

174 Although Li isotope fractionation and the magnesite:dolomite ratio of the precipitated solid both co-vary with temperature,

175 there is no relationship between the δ^7Li composition of the precipitated solids or that of their respective reactive solutions

176 and the magnesite:dolomite ratio of the precipitated solid (not shown). This suggests that the nature of the Ca-Mg carbonate

177 precipitated does not have a significant influence on Li isotope fractionation. This hypothesis is supported by the absence of

178 significant variation in the Li isotope fractionation factor ($10^3.ln\alpha_{prec-sol}$; Fig. 2) or the Li distribution coefficient between

6

179 solid and solution ($D_{[Li]prec-sol}$; Fig. 3), despite a wide range of mineral abundances. For instance, most $10^3.ln\alpha_{prec-sol}$

180 values are within error of each other while dolomite concentration varies from 17 to 82 wt % (Fig. 2a). This differs from what

181 Marriott et al. (2004b) observed for calcium carbonates at ambient temperature, where the isotopic fractionation is aragonite

182 ($\sim$11 ‰) was much greater than in calcite ($\sim$3 ‰).

183   The relationship between $10^3.ln\alpha_{prec-sol}$ and temperature can be used to estimate the temperature dependency for Li iso-

184 tope fractionation between Ca-Mg carbonate and solution. Using average $10^3.ln\alpha_{prec-sol}$ values for each reaction temperature,

185 we obtain the following temperature-dependent relationship:

186     $$10^3.ln\alpha_{prec-sol} = -((2.56 \pm 0.27).10^6)/T^2 + (5.8 \pm 1.3) \tag{3}$$

187   where T is the temperature of precipitation in K.

188   Using Eq. (3), the Li isotopic fractionation at 25 °C is estimated to be -23.0 $\pm$ 5.7 ‰ (1σ) (Fig. 4). Although there is a

189 large error on this estimate, our results suggest that Li isotopic fractionation during dolomite/magnesite precipitation is sig-

190 nificantly larger than during calcium carbonate precipitation (Marriott et al., 2004a). This temperature dependant relationship

191 of Li isotope fractionation in our high temperature experiments follows the isotope fractionation approach considering equi-

192 librium fractionation (Hoefs, 2015). Furthermore, we see that at high temperature [6]Li is preferentially incorporated into the

193 mineral phase over [7]Li, similar to what has been observed at low temperature for calcium carbonate (Marriott et al., 2004a,

194 b). Finally, despite a wide range of formation conditions between high-temperature synthetic dolomites and low-temperature

195 natural dolomites, Kaczmarek and Sibley (2007) showed that natural and synthetic dolomite form by the same growth mecha-

196 nisms. This was suggested through identification of identical growth features in etched natural and synthetic dolomite samples

197 as well as unetched synthetic dolomite. The growth fabrics of high-temperature synthetic dolomite and low-temperature nat-

198 ural dolomite have also been compared by Bullen and Sibley (1984), these results suggest that high-temperature synthetic

199 dolomites produce fabrics similar to that of naturally grown dolomites. Altogether, these observations suggest that the rela-

200 tionship between Li isotope fractionation and temperature derived from high temperature experiments may also be valid at low

201 temperatures characteristic of natural environments.

202   If the temperature of the solution from which dolomite is precipitated is known or can be calculated (e.g., via clumped

203 Δ_{47} proxy; Winkelstern et al. (2016)), the above relationship in combination with the δ^7Li of dolostone could potentially

204 be used to determine an estimate for the Li isotopic composition of the precipitating palaeo-solution , e.g. brine or seawater.

205 It is important to note that the applicability to natural systems may be limited to dolomite precipitated inorganically, while

206 it has been proposed that bacterial mediation could play a major role in the precipitation of dolomite from natural waters

207 at ambient conditions (Vasconcelos et al., 1995). Bacterial mediation was invoked to solve the "dolomite problem", i.e. the

208 inability to precipitate dolomite at ambient temperatures; the topic of the origin of dolomite formation still being hotly debated

209 (Liu et al., 2019; Ahm et al., 2019; Gregg et al., 2015). Other models invoke a primary or secondary (diagenetic) origin for

210 dolomite. Primary marine deposition has been invoked for dolomite formation in many studies, even in Precambrian dolostones

(Fairchild and Kennedy, 2007; Rose and Maloof, 2010; Kunzmann et al., 2013; Liu et al., 2014). Thus, where it can be shown that dolomite is of primary origin, its Li isotopic composition could provide valuable information on palaeo-environments.

4.2   Extraction of carbonate-bound Li in dolostones

Leaching of dolostone with solutions of variable HCl concentrations yields δ^7Li compositions of the leaching solution that decrease with increasing HCl concentrations, suggesting an increasing contribution of isotopically light Li from detrital silicates, such as clay minerals (Fig. 5a). This hypothesis is supported by a negative relationship between δ^7Li values and Li/Ca ratios of the leaching solutions (Fig. 6), similarly to results from leaching experiments on the Plenus Marl Limestone (Pogge von Strandmann et al., 2013). The Li/Ca ratio is used instead of Li/Mg because Mg is also present in silicate minerals. Indeed, δ^7Li and Li/Mg ratios show a positive relationship (Fig. 8b), surprisingly suggesting that dolomite and the detrital component are characterised by high and low Li/Mg ratios, respectively.

The increasing contribution of silicate minerals with the increasing HCl concentration of the leaching solution is further illustrated by increasing Al/Mg ratios in the leaching solution (Fig. 5b). The contribution from silicates becomes significant for HCl concentrations >0.5 M. For HCl concentrations <0.8 M, the relationship between Al/Mg and HCl concentration breaks down (Fig. 5b), indicating that silicates have a negligible role on the composition of the solution. Nevertheless, δ^7Li values decrease for HCl concentrations as low as 0.1 M. Thus, we propose that treatment of dolostone with a solution of 0.05 M HCl at room temperature for 60 mins, is the best compromise between minimising the contribution of silicates and obtaining enough Li for isotopic analysis.

Leaching experiments were also conducted on a *Porites* coral of Holocene age to test the proposed protocol, since the δ^7Li of modern coral is known (Marriott et al., 2004a; Rollion-Bard et al., 2009). Furthermore, because the aragonitic skeleton of modern corals is generally free of detrital material, we can also test that the chosen leaching protocol yields the same Li isotopic composition in the resulting solution, as with total dissolution of the coral. Total dissolution of the modern coral yields a δ^7Li value of 20.6 ‰ (Fig. 8). Leaching solutions with HCl concentrations <0.5 M HCl exhibit δ^7Li values within error of that obtained from total dissolution. These values are also consistent with δ^7Li compositions between 18.4 and 19.6 ‰ measured in *Porites*, and 21 ‰ in *Acropora* corals (Marriott et al., 2004a). Biomineralization has no major effect on the incorporation of Li in coral or foraminifera as Li has no known biological function. The Li isotopic difference between coral and seawater is -11 ‰ (Marriott et al., 2004a). Therefore, δ^7Li values obtained from the total dissolution and for leaching solutions with a HCl concentration <0.5 M would yield a δ^7Li composition for modern seawater of 31‰, consistent with published values (Misra and Froelich, 2012). Consequently, these results, which are similar to that of Dellinger et al., (2018) suggest that leaching with a 0.05 M HCl solution is appropriate to derive the Li associated to the carbonate fraction only.

Interestingly both coral and dolostone leaching solutions show a decrease in δ^7Li values with increasing HCl concentration. This is surprising since the coral is at 97 % aragonite (2 % magnesite and 1 % calcite) so the release of isotopically light Li from silicates is not expected. These results imply that total dissolution in dilute HNO_3 does not release isotopically light Li into solution, which could be contained in organic colloids, since no residue was observed. The lack of relationship between δ^7Li values and Li/Ca ratios (Fig. A1) suggests that this isotopically light Li is not bound to silicates (which would have a very

245 different Li/Ca from aragonite). In the coral, this pool of Li remains unidentified. However, as shown above, leaching with
246 solutions with <0.5 M HCl yield Li isotope compositions expected for a coral in equilibrium with the modern seawater.

247   Leaching of dolostone with acetic acid yields δ^7Li compositions in the solution similar to that of solutions with a HCl
248 concentration $\leq$0.1 M (Fig. 7). The δ^7Li composition of the 2 % HAc solution is lower (8.37 ‰) than that of the 0.5 % HAc
249 solution, which could maybe suggest a contribution from silicate-bound Li. Thus, treatment of dolostone with a solution of 0.5
250 % HAc at room temperature for 60 mins could be an alternative method to derive carbonate-bound Li.

5   Summary and Conclusions

252 Precipitation experiments at high temperature (150, 180 and 220 °C) yielded dolomite and magnesite in variable proportions.
253 However, varying mineralogy does not seem to measurably impact Li isotopic fractionation between the carbonate and the
254 solution. The Li isotopic composition of the precipitated solid is isotopically lighter than the reactive solution, similarly to
255 previous experiments on calcium carbonates (Marriott et al., 2004b, a). The isotope fractionation factor is mainly controlled
256 by temperature, which in turn allows us to calculate the Li isotopic composition of the solution using δ^7Li value of the Ca-
257 Mg carbonate, if the precipitation temperature can be estimated independently (e.g. oxygen or clumped isotope thermometry).
258 Thus, the temperature dependent relationship in Eq. (3) could be useful for reconstructing δ^7Li of palaeo-dolomitizing fluids
259 (i.e., reactive solution) as an approximation based on the Li isotope composition of dolostones in geological records.

260   Leaching experiments show that it is possible to selectively dissolve the carbonate-bound Li in dolostones by using 0.05 M
261 HCl or 0.5 % acetic acid at room temperature for 60 min. Leaching of coral with 0.05M HCl shows that this protocol yields a
262 Li isotope composition for the solution representative of that of the carbonate minerals. Thus, the described protocol allows us
263 to derive the Li isotope composition of the carbonate fraction of dolostones while leaving the Li from any co-present silicates
264 intact.

265   Combined results from leaching and precipitation experiments show that future studies of Li isotopes in dolostones have con-
266 siderable potential to further constraints the evolution of the Li isotopic composition of ancient precipitation fluids, including
267 seawater and basinal fluids, thus improve our understanding of changes in the Earth's palaeo-environments.

Table A1. Column calibration using seawater samples

Column ID	δ^7Li (‰)
Column A	31.1 ± 0.08
Column C	20.9 ± 0.08
Column D	31.6 ± 0.1
Column E	29.9 ± 0.08
Column F	31.7 ± 0.1
Column G	29.5 ± 0.07
Column H	30.7 ± 0.1
Column I	30.9 ± 0.1
Column J	30.9 ± 0.09
Column K	30.8 ± 0.09
Column L	32.0 ± 0.1
Column M	31.3 ± 0.1
Column N	30.7 ± 0.1
Column O	30.1 ± 0.1
Column P	30.8 ± 0.06
Column Q	30.6 ± 0.07
Column R	28.8 ± 0.08
Column S	31.1 ± 0.09
Column Z	29.3 ± 0.08

Errors are internal analytical
uncertainties reported at the 2σ level.
Column C was not used due to the
δ^7Li value being significantly
different from the seawater value.

Table A2. Concentrations of lithium in reactive fluids and precipitated solids

Sample ID	$[Li]_{sol}$ ($\mu g.L^{-1}$)	$[Li]_{prec}$ (ppm)
LiDol-150-4.1	3,695	25.9
LiDol-150-4.2	3,415	20.5
LiDol-150-4.3	3,036	21.8
LiDol-180-4.1	3,434	16.0
LiDol-180-4.2	3,238	15.7
LiDol-220-3	1,666	8.20

Table A3. Mineral concentration of Nuccaleena dolostone (EC26) used in the leaching experiment

Mineral	Concentration (wt%)
Quartz	14
Albite	5.1
Calcite	1.1
Dolomite	70
Ankerite	2.1
Siderite	0.2
Kaolinite	1.0
Chlorite	0.2
Muscovite	6.2

Table A4. Mineral concentrations of coral used in the leaching experiment

Mineral	Concentration (wt%)
Aragonite	97
Calcite	1.0
Dolomite	0.4
Magnesite	1.6

References

Ahm, A.-S. C., Maloof, A. C., Macdonald, F. A., Hoffman, P. F., Bjerrum, C. J., Bold, U., Rose, C. V., Strauss, J. V., and Higgins, J. A.: An early diagenetic deglacial origin for basal Ediacaran "cap dolostones", Earth and Planetary Science Letters, 506, 292–307, https://doi.org/10.1016/J.EPSL.2018.10.046, https://www.sciencedirect.com/science/article/pii/S0012821X18306484, 2019.

Arvidson, R. S. and Mackenzie, F. T.: The dolomite problem; control of precipitation kinetics by temperature and saturation state, American Journal of Science, 299, 257–288, 1999.

Balter, V. and Vigier, N.: Natural variations of lithium isotopes in a mammalian model, Metallomics, 6, 582–586, https://doi.org/10.1039/C3MT00295K, http://dx.doi.org/10.1039/C3MT00295K, 2014.

Bastian, L., Vigier, N., Reynaud, S., Kerros, M.-E., Revel, M., and Bayon, G.: Lithium Isotope Composition of Marine Biogenic Carbonates and Related Reference Materials, Geostandards and Geoanalytical Research, 42, 403–415, https://doi.org/10.1111/ggr.12218, http://doi.wiley.com/10.1111/ggr.12218, 2018.

Bullen, S. B. and Sibley, D. F.: Dolomite selectivity and mimic replacement, Geology, 12, 655, https://doi.org/10.1130/0091-7613(1984)12<655:DSAMR>2.0.CO;2, https://pubs.geoscienceworld.org/geology/article/12/11/655-658/188317, 1984.

Burns, S. J., Mckenzie, J. A., and Vasconcelos, C.: Dolomite formation and biogeochemical cycles in the Phanerozoic, Sedimentology, 47, 49–61, 2000.

Carignan, J., Vigier, N., and Millot, R.: Three secondary reference materials for lithium isotope measurements: Li7-N, Li6-N and LiCl-N solutions, Geostandards and Geoanalytical Research, 31, 7–12, 2007.

Dellinger, M., West, A. J., Paris, G., Adkins, J. F., von Strandmann, P. A. P., Ullmann, C. V., Eagle, R. A., Freitas, P., Bagard, M.-L., and Ries, J. B.: The Li isotope composition of marine biogenic carbonates: Patterns and Mechanisms, Geochimica et Cosmochimica Acta, 2018.

Fairchild, I. J. and Kennedy, M. J.: Neoproterozoic glaciation in the Earth System, Journal of the Geological Society, 164, 895–921, https://doi.org/10.1144/0016-76492006-191, http://jgs.lyellcollection.org/lookup/doi/10.1144/0016-76492006-191, 2007.

Flesch, G. D., Anderson, A. R., and Svec, H. J.: A secondary isotopic standard for 6Li/7Li determinations, International Journal of Mass Spectrometry and Ion Physics, 12, 265–272, 1973.

Geske, A., Zorlu, J., Richter, D., Buhl, D., Niedermayr, A., and Immenhauser, A.: Impact of diagenesis and low grade metamorphism on isotope (δ^{26}Mg, δ^{13}C, δ^{18}O and ^{87}Sr/^{86}Sr) and elemental (Ca, Mg, Mn, Fe and Sr) signatures of Triassic sabkha dolomites, Chemical Geology, 332, 45–64, 2012.

Gregg, J. M., Bish, D. L., Kaczmarek, S. E., and Machel, H. G.: Mineralogy, nucleation and growth of dolomite in the laboratory and sedimentary environment: A review, Sedimentology, 62, 1749–1769, https://doi.org/10.1111/sed.12202, http://doi.wiley.com/10.1111/sed.12202, 2015.

Hathorne, E. C. and James, R. H.: Temporal record of lithium in seawater: A tracer for silicate weathering?, Earth and Planetary Science Letters, 246, 393–406, http://www.scopus.com/inward/record.url?eid=2-s2.0-33747107536&partnerID=40&md5=eaa584abda4cb4fe510137c52bc40355https://ac-els-cdn-com.ezproxy.uow.edu.au/S0012821X06003086/1-s2.0-S0012821X06003086-main.pdf?_tid=2497a4da-cd95-11e7-9ebf-00000aacb35d&acdnat=1511142790_96f8e94acb3fcc4519433bade7e2c481, 2006.

Hoefs, J.: Theoretical and Experimental Principles, in: Stable Isotope Geochemistry, pp. 1–46, Springer International Publishing, Cham, https://doi.org/10.1007/978-3-319-19716-6_1, http://link.springer.com/10.1007/978-3-319-19716-6{_}1, 2015.

314   James, R. H. and Palmer, M. R.: The lithium isotope composition of international rock standards, Chem. Geol., 166, 319–326, 2000.

315   Kaczmarek, S. E. and Sibley, D. F.: A Comparison of Nanometer-Scale Growth and Dissolution Features on Natural and Synthetic Dolomite

316   Crystals: Implications for the Origin of Dolomite, Journal of Sedimentary Research, 77, 424–432, https://doi.org/10.2110/jsr.2007.035,

317   https://pubs.geoscienceworld.org/jsedres/article/77/5/424-432/145154, 2007.

318   Kazuyo Yamaji, Yoji Makita, Hidekazu Watanabe, Akinari Sonoda, Hirofumi Kanoh, ., , Takahiro Hirotsu, and Ooi*, K.: Theoretical Esti-

319   mation of Lithium Isotopic Reduced Partition Function Ratio for Lithium Ions in Aqueous Solution, https://doi.org/10.1021/JP001303I,

320   https://pubs.acs.org/doi/abs/10.1021/jp001303i, 2001.

321   Kunzmann, M., Halverson, G. P., Sossi, P. A., Raub, T. D., Payne, J. L., and Kirby, J.: Zn isotope evidence for immediate resumption of

322   primary productivity after snowball Earth, Geology, 41, 27–30, https://doi.org/10.1130/g33422.1, http://geology.gsapubs.org/content/41/

323   1/27.abstract, 2013.

324   Land, L. S.: Failure to precipitate dolomite at 25 degrees C from dilute solution despite 1000-fold oversaturation after 32 years, Aquatic

325   Geochemistry, 4, 361–368, https://doi.org/10.1023/A:1009688315854, 1998.

326   Lechler, M., Pogge von Strandmann, P. A. E., Jenkyns, H. C., Prosser, G., and Parente, M.: Lithium-isotope evidence for

327   enhanced silicate weathering during OAE 1a (Early Aptian Selli event), Earth and Planetary Science Letters, 432, 210–

328   222, https://doi.org/http://dx.doi.org/10.1016/j.epsl.2015.09.052, http://www.sciencedirect.com/science/article/pii/S0012821X15006299,

329   2015.

330   Li, D. D., Jacobson, A. D., and McInerney, D. J.: A reactive-transport model for examining tectonic and climatic con-

331   trols on chemical weathering and atmospheric CO2 consumption in granitic regolith, Chemical Geology, 365, 30–42,

332   https://doi.org/http://dx.doi.org/10.1016/j.chemgeo.2013.11.028, http://www.sciencedirect.com/science/article/pii/S0009254113005664,

333   2014.

334   Liu, C., Wang, Z., Raub, T. D., Macdonald, F. A., and Evans, D. A. D.: Neoproterozoic cap-dolostone deposition in stratified glacial meltwater

335   plume, Earth and Planetary Science Letters, 404, 22–32, https://doi.org/10.1016/j.epsl.2014.06.039, 2014.

336   Liu, D., Xu, Y., Papineau, D., Yu, N., Fan, Q., Qiu, X., and Wang, H.: Experimental evidence for abiotic formation of low-temperature

337   proto-dolomite facilitated by clay minerals, Geochimica et Cosmochimica Acta, 247, 83–95, https://doi.org/10.1016/J.GCA.2018.12.036,

338   https://www.sciencedirect.com/science/article/pii/S0016703718307257, 2019.

339   Marriott, C. S., Henderson, G. M., Belshaw, N. S., and Tudhope, A. W.: Temperature dependence of δ^7Li, δ^{44}Ca and Li/Ca during growth

340   of calcium carbonate, Earth and Planetary Science Letters, 222, 615–624, 2004a.

341   Marriott, C. S., Henderson, G. M., Crompton, R., Staubwasser, M., and Shaw, S.: Effect of mineralogy, salinity, and temperature on Li/Ca

342   and Li isotope composition of calcium carbonate, Chemical Geology, 212, 5–15, 2004b.

343   Misra, S. and Froelich, P. N.: Lithium isotope history of Cenozoic seawater: Changes in silicate weathering and reverse weathering, Science,

344   335, 818–823, https://doi.org/DOI 10.1126/science.1214697, <GotoISI>://000300356400035, 2012.

345   Pistiner, J. S. and Henderson, G. M.: Lithium-isotope fractionation during continental weathering processes, Earth and Planetary Science

346   Letters, 214, 327–339, https://doi.org/10.1016/s0012-821x(03)00348-0, 2003.

347   Pogge von Strandmann, P. A. E., Jenkyns, H. C., and Woodfine, R. G.: Lithium isotope evidence for en-

348   hanced weathering during Oceanic Anoxic Event 2, Nature Geosci, 6, 668–672, https://doi.org/10.1038/ngeo1875

349   http://www.nature.com/ngeo/journal/v6/n8/abs/ngeo1875.html#supplementary-information, http://dx.doi.org/10.1038/ngeo1875, 2013.

Pogge von Strandmann, P. A. E., Desrochers, A., Murphy, M. J., Finlay, A. J., Selby, D., and Lenton, T. M.: Global climate stabilisation by chemical weathering during the Hirnantian glaciation, Geochemical Perspectives Letters, pp. 230–237, https://doi.org/10.7185/geochemlet.1726, 2017.

Rollion-Bard, C., Vigier, N., Meibom, A., Blamart, D., Reynaud, S., Rodolfo-Metalpa, R., Martin, S., and Gattuso, J.-P.: Effect of environmental conditions and skeletal ultrastructure on the Li isotopic composition of scleractinian corals, Earth and Planetary Science Letters, 286, 63–70, https://doi.org/10.1016/j.epsl.2009.06.015, 2009.

Rose, C. V. and Maloof, A. C.: Testing models for post-glacial 'cap dolostone' deposition: Nuccaleena Formation, South Australia, Earth and Planetary Science Letters, 296, 165–180, https://doi.org/10.1016/j.epsl.2010.03.031, 2010.

Teng, F. Z., Dauphas, N., and Helz, R. T.: Iron Isotope Fractionation During Magmatic Differentiation in Kilauea Iki Lava Lake, Science, 320, 1620–1622, https://doi.org/10.1126/science.1157166, 2008.

Vasconcelos, C., McKenzie, J. A., Bernasconi, S., Grujic, D., and Tiens, A. J.: Microbial mediation as a possible mechanism for natural dolomite formation at low temperatures, Nature, 377, 220, https://doi.org/10.1038/377220a0, http://dx.doi.org/10.1038/377220a0http://www.nature.com/articles/377220a0, 1995.

Vigier, N. and Goddéris, Y.: A new approach for modeling Cenozoic oceanic lithium isotope paleo-variations: the key role of climate, Climate of the Past, 11, 635–645, https://doi.org/10.5194/cp-11-635-2015, 2015.

Wanner, C., Sonnenthal, E. L., and Liu, X.-M.: Seawater δ^7Li: A direct proxy for global CO2 consumption by continental silicate weathering?, Chemical Geology, https://doi.org/http://dx.doi.org/10.1016/j.chemgeo.2014.05.005, http://www.sciencedirect.com/science/article/pii/S0009254114002435, 2014.

Winkelstern, I. Z., Kaczmarek, S. E., Lohmann, K. C., and Humphrey, J. D.: Calibration of dolomite clumped isotope thermometry, Chemical Geology, 443, 32–38, https://doi.org/10.1016/j.chemgeo.2016.09.021, http://dx.doi.org/10.1016/j.chemgeo.2016.09.021, 2016.
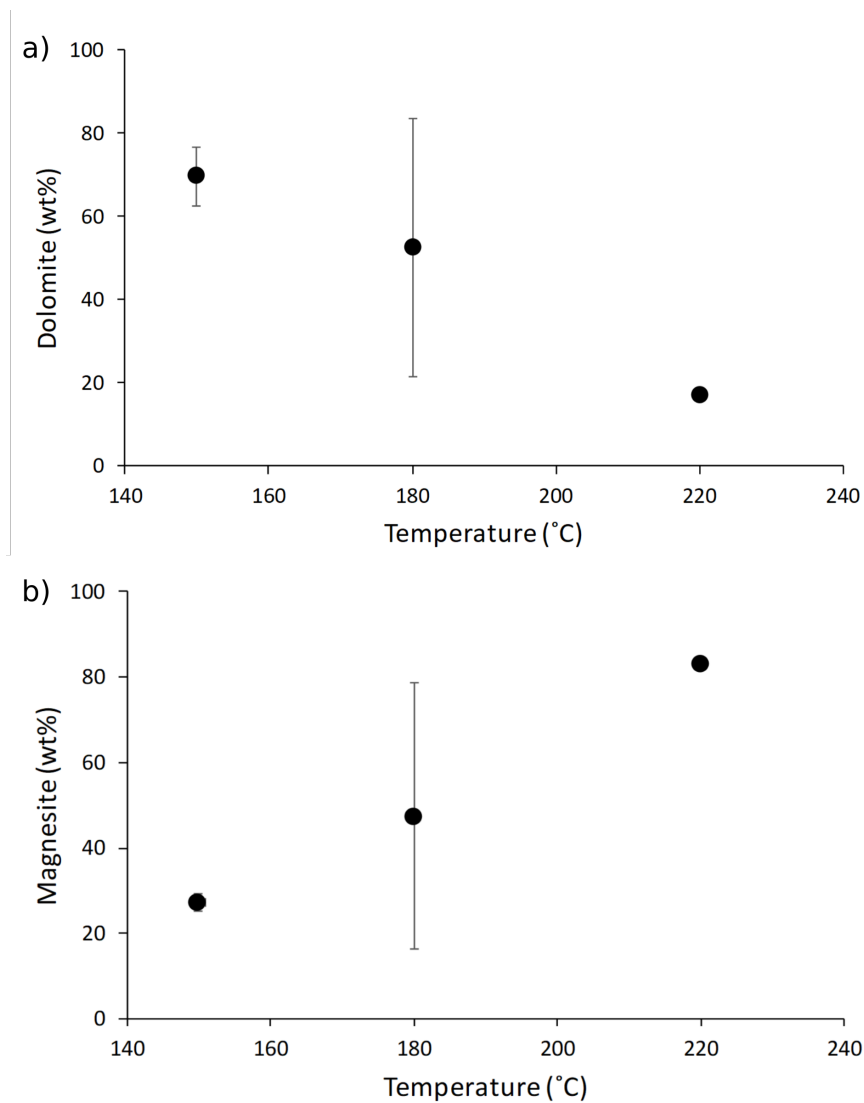
Figure 1. a) Dolomite and b) magnesite concentrations in the precipitated solid (in wt %) as function of reaction temperature (in °C). The data displayed are average values for each reaction temperature. Error is not shown for mineral concentrations at 220 °C because no repeat analysis was performed. The error on the magnesite content at 150 °C is within the symbol size.
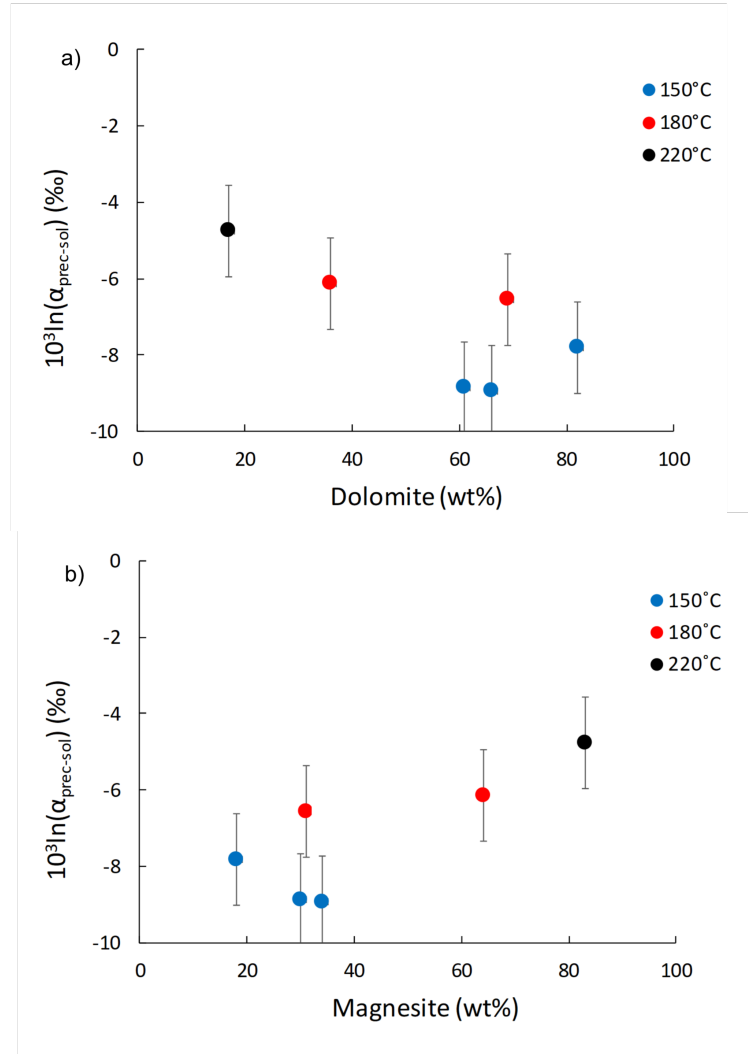
Figure 2. Lithium isotope fractionation factor between the precipated solid and the solution ($10^3.ln\alpha_{prec-sol}$) as a function of a) dolomite and b) magnesite contents (in wt %).

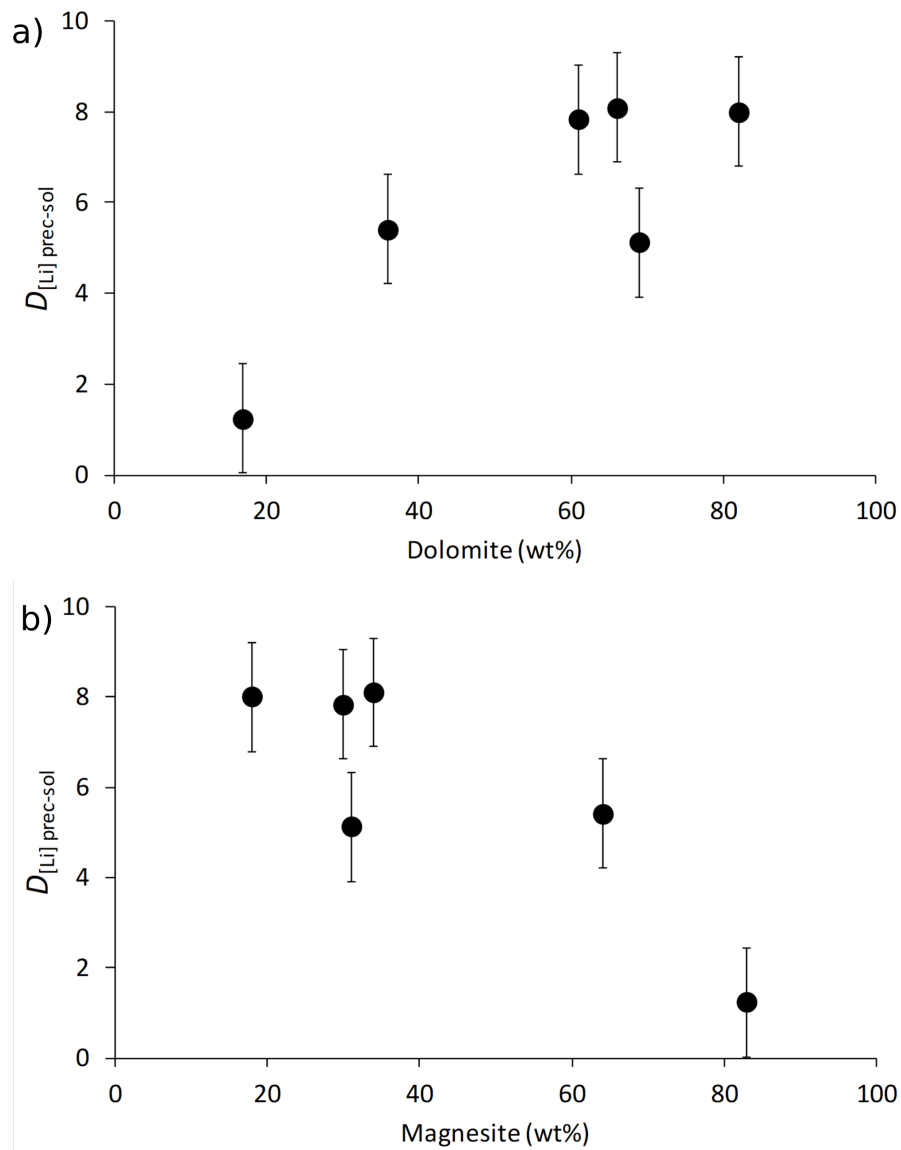**Figure 3.** The distribution coefficent of Li between solid and solution ($D_{[Li]prec-sol}$) as a function of a) dolomite and b) magnesite contents (in wt %).
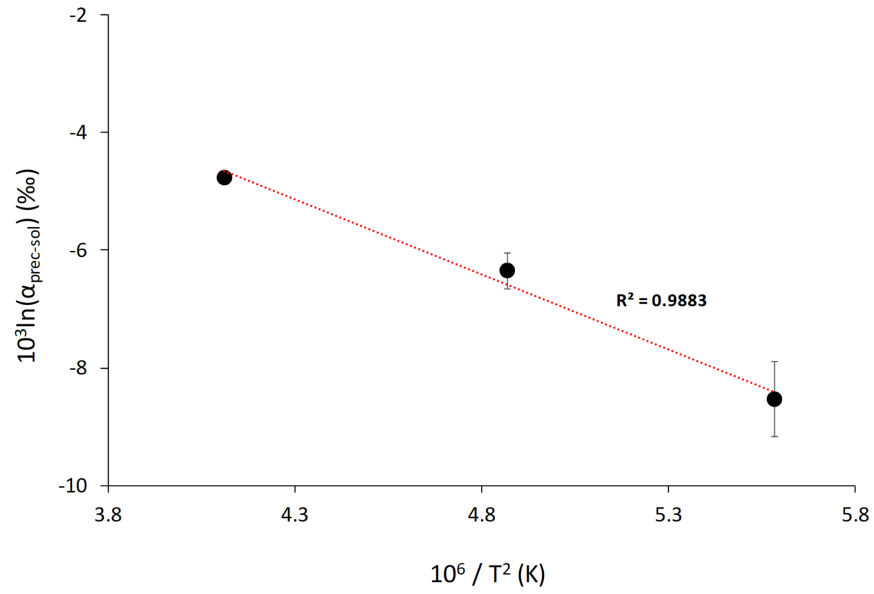
Figure 4. Lithium isotope fractionation factor as a function of the reaction temperature, T (in K). Average values for each temperature are shown. The dotted line shows the linear regression through these values according to Eq. (3). Error is not shown for the isotope fractionation factor at 220 °C because no repeat analysis was performed.
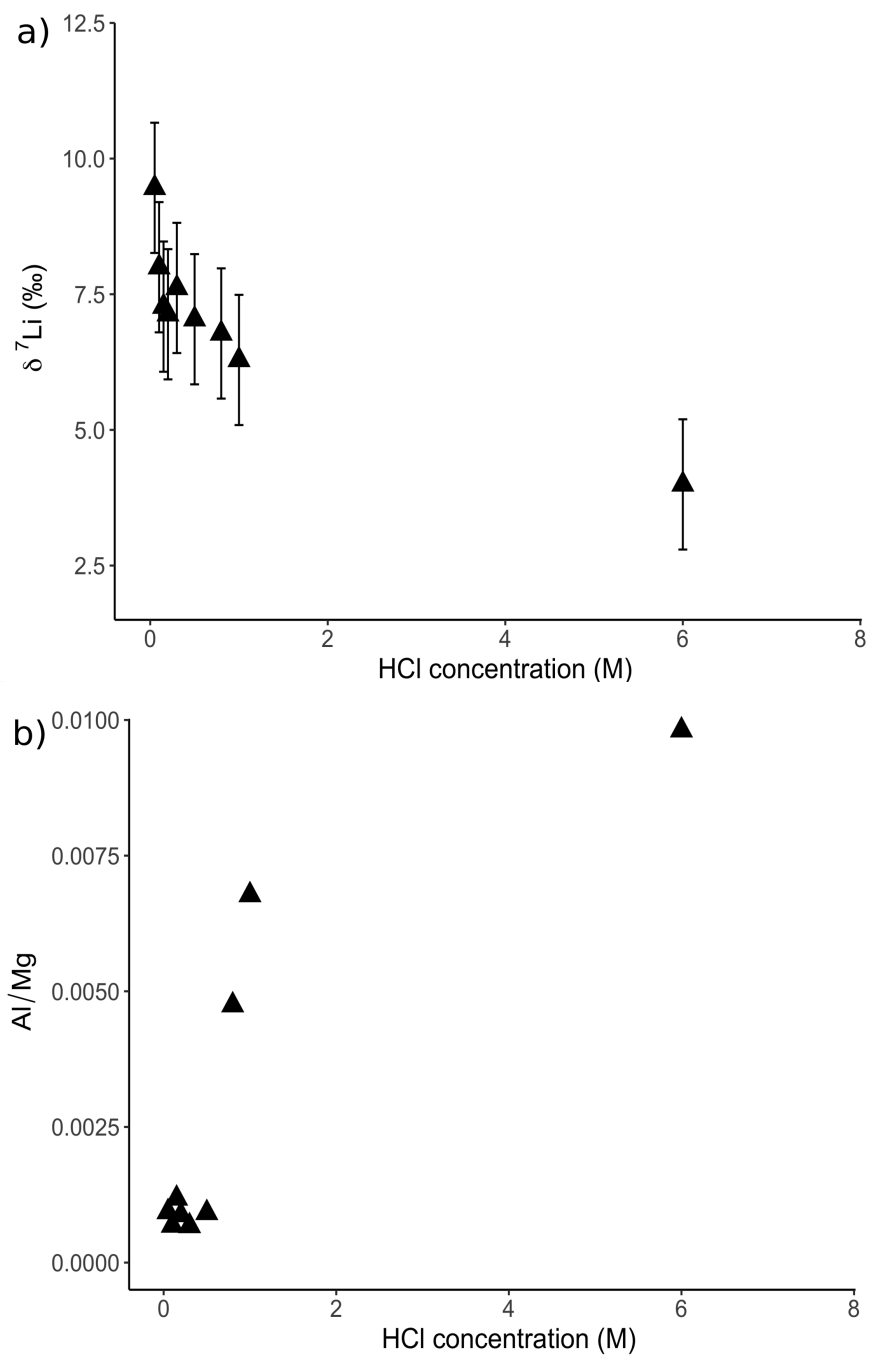
Figure 5. a) Lithium isotope compositions and b) Al/Mg ratios of solutions from dolostone leaching, as a function of their HCl concentration. Decreasing δ^7Li values with increasing HCl concentration suggest a release of isotopically light Li from clay minerals, which is supported by the increase in Al/Mg ratios. Error bars are within the symbol size, if not shown.
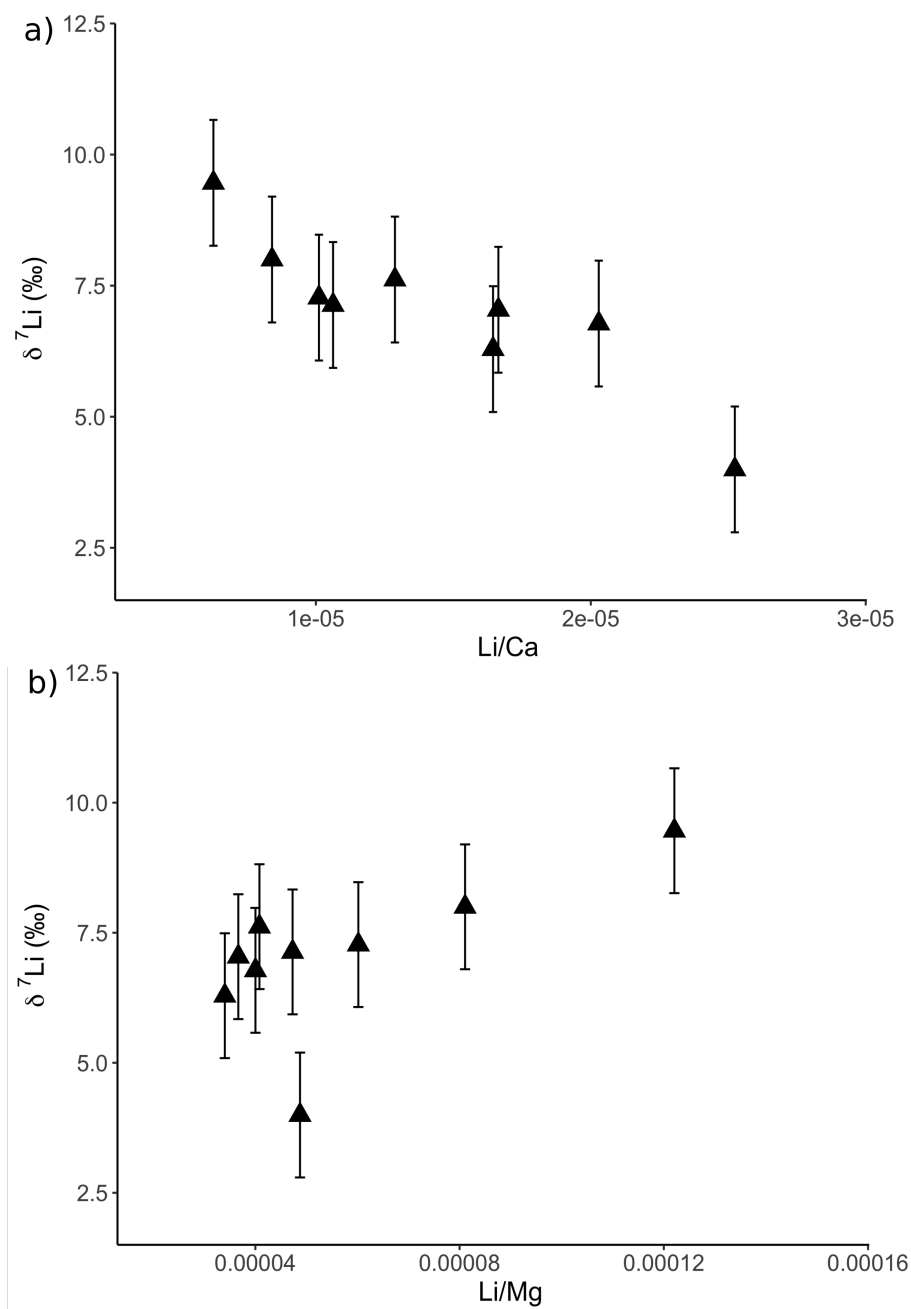
Figure 6. Lithium isotopic compositions of solutions from dolostone leaching, as a function of their (a) Li/Ca and b) Li/Mg ratios. Error bars are within the symbol size, if not shown.
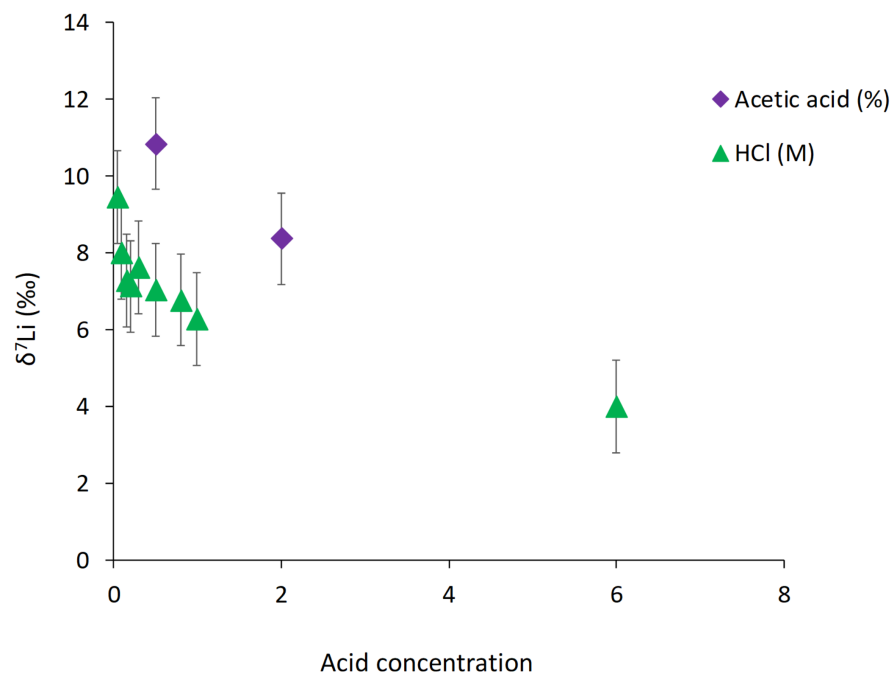
Figure 7. Lithium isotope composition of leaching solutions for experiments with HCl and acetic acid.
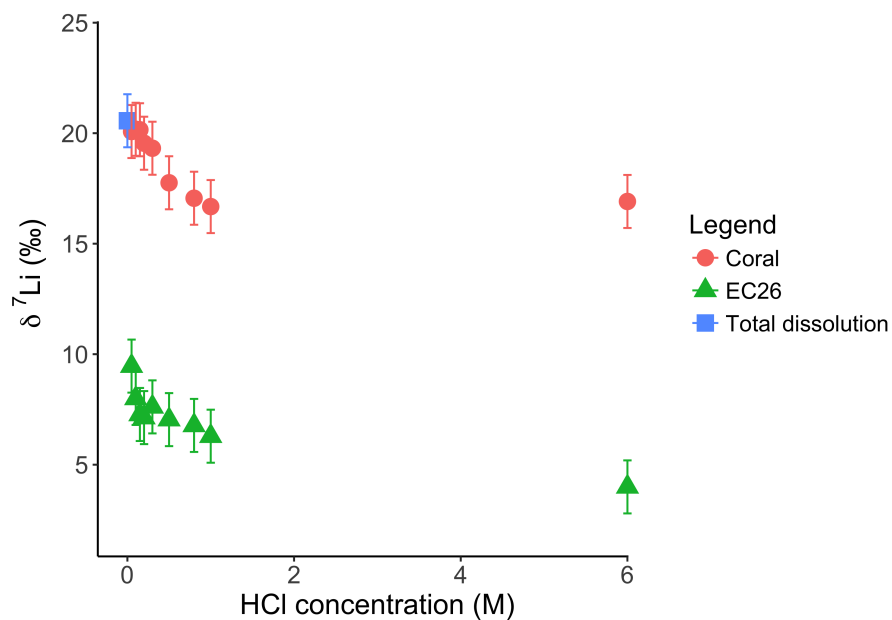
Figure 8. Lithium isotope composition of leaching solutions as a function of their HCl concentrations. Triangles and circles show the composition of solutions used to leach a Neoproterozoic dolostone and a modern coral, respectively. The square shows the composition of the coral total dissolution. Both coral and dolostone solutions show similar trends, suggesting release of silicate-bound Li at higher HCl concentrations. This is surprising since the coral is almost exclusively aragonite, so the release of isotopically light Li is not expected. This also implies that total dissolution in dilute HNO_3 does not release isotopically light Li into solution, although no residue was observed during dissolution in dilute HNO_3.
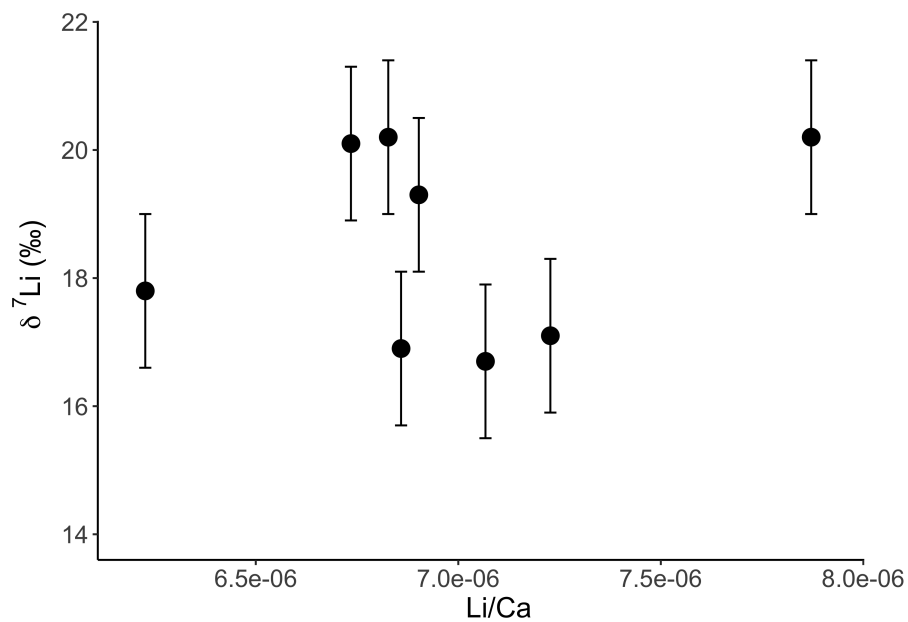
Figure A1. Lithium isotope composition of solutions from coral leaching, as a function of their Li/Ca ratio. Unlike for the dolostone, there is no relationship between δ^7Li and Li/Ca. This could indicate that the isotopically-light Li is bound to a fraction with a Li/Ca similar to that of aragonite. Error bars are within the symbol size, if not shown.

Tables

Table 1. Reaction temperatures and mineral content from the precipitation experiments

Sample ID	Reaction time (days)	T (°C)	magnesite	dolomite	dolomite: magnesite
LiDol – 150 – 4.1	150	150	18.0	82.0	4.56
LiDol – 150 – 4.2	150	150	34.0	66.0	1.94
LiDol – 150 – 4.3	150	150	30.0	61.0	2.03
LiDol – 180 – 4.1	150	180	31.0	69.0	2.23
LiDol – 180 – 4.2	150	180	64.0	36.0	0.56
LiDol – 220 – 3	100	220	83.0	17.0	0.20

Mineral content in wt %. Note a maximum reaction time of 100 days was only possible at 220 °C, since no reacting solution was left after this time.

Table 2. Li isotope compositions solutions and precipitated solids for the precipitation experiments

Sample ID	Temperature (°C)	δ^7Li solution (‰)	δ^7Li solid (‰)	$10^3 ln(\alpha_{prec-sol})$	$D_{[Li]prec-sol}$
LiCl reactive solution	-	7.85	-	-	-
LiDol – 150 – 4.1	150	7.87	0.03	-7.81	7.01
LiDol – 150 – 4.2	150	8.34	-0.63	-8.93	6.00
LiDol – 150 – 4.3	150	8.79	-0.10	-8.86	7.19
LiDol – 180 – 4.1	180	9.48	2.88	-6.56	4.66
LiDol – 180 – 4.2	180	7.88	1.71	-6.14	4.85
LiDol – 220 – 3	220	7.87	3.08	-4.77	4.92

External uncertainty (at the 2 σ level) is 0.86 and 1.2 ‰ on the δ^7Li values of precipitated solids and solutions, respectively.

Table 3. Lithium isotope compositions and elemental concentrations of solutions from the dolostone and coral leaching experiments with HCl and HAc

HCl concentration (M)	δ^7Li$_d$ (‰)	δ^7Li$_c$ (‰)	Al (ppb)	Li (ppb)	Mg (ppm)	Ca (ppm)
0.05	9.46	20.1	151.0	19.8	162.0	3151.1
0.10	8.00	20.2	241.5	28.6	353.3	3407.1
0.15	7.27	20.2	637.4	32.4	538.9	3206.8
0.20	7.13	19.5	712.3	38.4	811.8	3612.8
0.30	7.62	19.3	848.9	51.3	1257.6	3984.8
0.50	7.04	17.8	2024.1	81.0	2209.0	4867.5
0.80	6.78	7.04	13588.1	114.6	2864.1	5649.2
1.00	6.29	16.7	21984.3	110.4	3245.4	6714.2
6.00	4.00	16.9	32541.9	161.7	3317.0	6406.7
total dissolution	n/a	20.6				
HAc concentration (%)	δ^7Li$_d$ (‰)					
0.5	10.9					
2	8.37					

δ^7Li$_d$ (‰) and δ^7Li$_c$ (‰) are the Li isotope composition of solutions from dolostone and coral leaching experiments, respectively.